Superconducting boron allotropes

Shoutao Zhang [1], Xin Du,[1] Jianyan Lin [1], Aitor Bergara [3,4,5,*], Xin Chen,[2] Xiaobing Liu,[2,†]
Xiaohua Zhang,[1] and Guochun Yang [1,‡]

[1]*Centre for Advanced Optoelectronic Functional Materials Research and Laboratory for UV Light-Emitting Materials and Technology of Ministry of Education, Northeast Normal University, Changchun 130024, China*

[2]*Laboratory of High Pressure Physics and Material Science, School of Physics and Physical Engineering, Qufu Normal University, Qufu, Shandong Province 273165, China*

[3]*Departamento de Física de la Materia Condensada, Universidad del País Vasco-Euskal Herriko Unibertsitatea, UPV/EHU, 48080 Bilbao, Spain*

[4]*Donostia International Physics Center (DIPC), 20018 Donostia, Spain*

[5]*Centro de Física de Materiales CFM, Centro Mixto CSIC-UPV/EHU, 20018 Donostia, Spain*

The search for elemental allotropes is an active research field to get unusual structures with unique properties. The removal of metal atoms from pressure-induced stable binary compounds has become a useful method for obtaining elemental allotropes with interesting properties that otherwise would not be accessible at ambient pressure. Although three-dimensional boron allotropes have been studied extensively, none of those found so far are superconducting at ambient pressure. Here we propose that NaB_4 and Na_2B_{17} can be used as precursors to achieve superconducting boron allotropes at ambient pressure. First-principle swarm-intelligence structure search calculations identify several novel sodium borides (e.g., Na_3B_2, Na_2B_3, NaB_4, and Na_2B_{17}) under high pressure. Interestingly, the B atoms in $I4/mmm$ NaB_4 and Pm Na_2B_{17} form three-dimensional frameworks with open channels, where Na atoms are located. After the removal of Na atoms, two hitherto unknown boron allotropes, named as $I4/mmm$ B_4 and Pm B_{17}, are stable at ambient pressure. They are metallic with superconducting critical temperatures of 19.8 and 15.4 K, respectively, becoming the highest ones among bulk boron allotropes. In addition, considering their predicted Vickers hardness of 27.3 and 26.8 GPa, they are also potential hard materials.

I. INTRODUCTION

The preparation of high-temperature superconductors is of great importance for fundamental research and practical applications [1–6]. Recently discovered pressure-induced stable H-rich compounds (e.g., H_3S [7] and LaH_{10} [8,9]) broke the superconducting transition temperature record of 164 K in cuprates [10]. Notably, theoretical predictions play a leading role in accelerating these innovative discoveries [11–13]. Very recently, room-temperature or even higher-temperature superconductivity has been predicted through doping lithium into MgH_{16}, forming a novel ternary compound, Li_2MgH_{16} [14]. However, a common characteristic of these hydrides is that their superconductivity emerges at more than one million times the atmospheric pressure. Therefore, the search for stable or metastable superconducting materials at ambient pressure is highly needed for practical application [15].

Some of pressure-induced stable compounds are recoverable to ambient pressure with interesting properties, especially for light mass elements, such as boron, carbon, and nitrogen.

They can be synthesized, since pressure allows them to overcome the required reaction barriers to be formed. For example, well-known superhard materials, such as BC_3 [16] and diamond [17], are synthesized at high pressures and become metastable at ambient pressure. On the other hand, pressure-induced stable binary compounds are also used as precursors to achieve elemental allotropes. For instance, two silicon allotropes, Si_{24} [18] and $P6/m$-Si_6 [19], are obtained through a two-step synthesis methodology, removing the Na atoms from the pressure-induced stable Na_4Si_{24} and $P6/m$-$NaSi_6$ via a thermal "degassing" process. More interestingly, Si_{24} has a proper band gap of 1.3 eV, showing broad applications as photovoltaic cells [18]. $P6/m$-Si_6 becomes a superconductor with a critical transition temperature of 12 K at ambient pressure [19]. In both structures the Si atoms form a three-dimensional frame with open channels, where the Na atoms are located, which makes it easy for them to escape.

The study of boron allotropes has attracted great attention because of their electron deficiency, structural complexity, and unusual bonding pattern [20,21]. Up to now, at least 14 boron allotropes have been reported [22]. Most of them consist of B_{12} icosahedra [23]. However, the arrangement of the icosahedra strongly modifies their electronic properties. For instance, $I2_12_12_1$-B_{60}, where B_{12} icosahedra are linked by helical boron chains, is a metal, whereas $Pnma$-B_{60}, in

*Corresponding author: a.bergara@ehu.eus

†Corresponding author: xiaobing.phy@qfnu.edu.cn

‡Corresponding author: yanggc468@nenu.edu.cn

which B_{12} icosahedra are interconnected by two-atom wide B ribbons, is a semimetal [24]. After compression, boron allotropes undergo complex structural transitions, caused by the appearance of novel boron units, which also modify their electronic properties [23,25–29]. So far, no bulk superconducting boron allotrope has been found at ambient pressure.

Having in mind that pressure can stabilize unusual stoichiometric compounds [30–32] and that known sodium borides consist of covalent B frames [33–35], we consider the binary Na-B system to explore stable B-rich Na-B compounds with open channel frames, then to obtain metastable boron allotropes after releasing Na atoms. In this work, first-principle swarm-intelligence structural search method was employed to identify stable Na-B compounds at high pressures. Besides reproducing the known Na-B compounds (e.g., Na_3B_{20} [33] and NaB_{15} [35]) at ambient pressure, four new Na-B compositions (e.g., Na_3B_2, Na_2B_3, NaB_4, and Na_2B_{17}) become stable under high pressure. As expected, two metastable $I4/mmm$ B_4 and Pm B_{17} allotropes are obtained from $I4/mmm$ NaB_4 and Pm Na_2B_{17} precursors. Interestingly, these new compounds are predicted to be highly stable and even superconductors, becoming the first superconducting bulk boron allotropes at ambient pressure.

II. COMPUTATIONAL METHODS

To explore the stable Na-B phases under high pressure, we employ a swarm-intelligence based CALYPSO structure search method [36,37], which can find stable structures just depending on the chemical compositions. The geometry optimization and calculations of the electronic properties are performed with the Vienna *ab initio* simulation package (VASP) code [38] within the framework of density functional theory (DFT) [39,40]. The all-electron projector augmented-wave (PAW) [41] pseudopotentials with $2s^2 2p^6 3s^1$ and $2s^2 2p^1$ valence electrons for Na and B atoms, respectively, are used to describe the interactions between electrons and ions. The full-potential all-electron calculations of the equation of states for NaB_4 compound were performed with the full-potential linearized augmented plane-wave method as implemented in the WIEN2K code [42] to examine the validity of the selected PAW pseudopotentials under high pressure (Fig. S0). The Perdew-Burke-Ernzerhof (PBE) [43] functional within the generalized gradient approximation (GGA) [44] is used to account for the exchange-correlation energy. A cutoff energy of 800 eV and a Monkhorst-Pack [45] k-point grid with a reciprocal space resolution of $2\pi \times 0.03$ Å^{-1} in the Brillouin zone yield an excellent convergence for the Gibbs free energy. Electron-phonon coupling calculations within the density functional perturbation theory and the plane-wave pseudopotential method with ultrasoft pseudopotentials are implemented in the QUANTUM ESPRESSO package [46]. More detailed illustrations of structure search and computational details can be found in the Supplemental Material [47].

III. RESULTS AND DISCUSSION

A. Phase stability

Here we mainly focused on B-rich Na-B compounds, which have a tendency to form three-dimensional B frames.
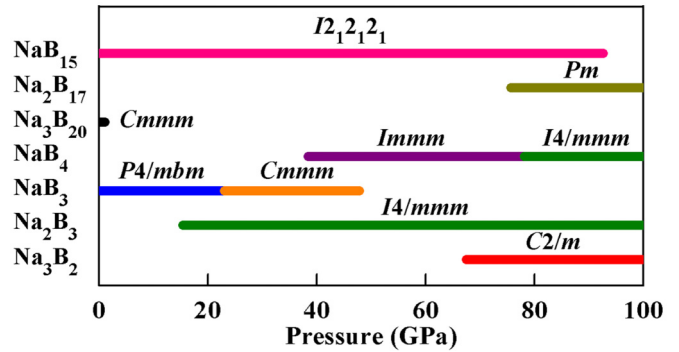

FIG. 1. Pressure-composition phase stability diagram of the Na-B system between 1 atm and 100 GPa.

We conduct an extensive structure search on Na-B compounds with a variety of $Na_m B_n$ ($m = 1$, $n = 1$–20; $m = 2$, $n = 1, 3, 5, 7, 9, 11, 13, 15, 17, 19$; $m = 3$, $n = 2, 20$) compositions at 0 K and the following pressures, 1 atm and 10, 25, 50, and 100 GPa. The relative thermodynamic stabilities of the considered $Na_m B_n$ compounds are shown in the convex hull diagram [48] (Fig. S1). The thermodynamic stable phases sitting at the solid line are denoted by solid spheres, whereas the metastable phases, represented by open spheres, decompose into elemental Na [49,50] and B [23] solids or other $Na_m B_n$ phases. At ambient pressure, the already known $Cmmm$ Na_3B_{20} and $I2_12_12_1$ NaB_{15} are reproduced in our structure search [35]. As can be seen in Fig. 1, $I2_12_12_1$ NaB_{15} shows a much larger stable pressure range than $Cmmm$ Na_3B_{20}. On the other hand, the predicted phases and phase transition pressures for NaB_3 are in excellent agreement with the results of Zhou *et al.* (Fig. S2) [34]. All these results demonstrate that our adopted structure search method and pseudopotentials are suitable for the Na-B system.

At higher pressures, several new B-rich stoichiometries (i.e., Na_2B_3, NaB_4, and Na_2B_{17}) emerge on the convex hull (Fig. S1). Their stable pressure ranges are shown in Fig. 1. In more detail, $I4/mmm$ Na_2B_3 is predicted to be stable above 15.4 GPa. For NaB_4, there are two stable phases in the pressure range considered: $Immm$ NaB_4 becomes stable at 38.4 GPa and then transforms into $I4/mmm$ NaB_4 above 78.1 GPa. Na_2B_{17}, with a higher B content, stabilizes above 75.6 GPa. Na-rich $C2/m$ Na_3B_2 begins to be stable above 67.5 GPa. For compounds containing light elements, zero-point energy (ZPE) potentially has a large contribution to the total Gibbs free energy, which might influence their relative stability [51–53]. However, the inclusion of ZPE for the predicted sodium borides at the selected pressure of 100 GPa did not change their relative stabilities (Fig. S3). Phonon spectra calculations [54,55] demonstrate that all $Na_m B_n$ compounds are dynamically stable, with no imaginary frequency modes at any high-symmetry direction in the whole Brillouin zone (Fig. S4).

B. Crystal structures

We mainly focus on the phases of NaB_4 and Na_2B_{17}, consisting of three-dimensional B frames. The structures and electron properties of the other predicted Na_3B_2 and Na_2B_3 can be found in Figs. S5 and S6. The low-pressure NaB_4
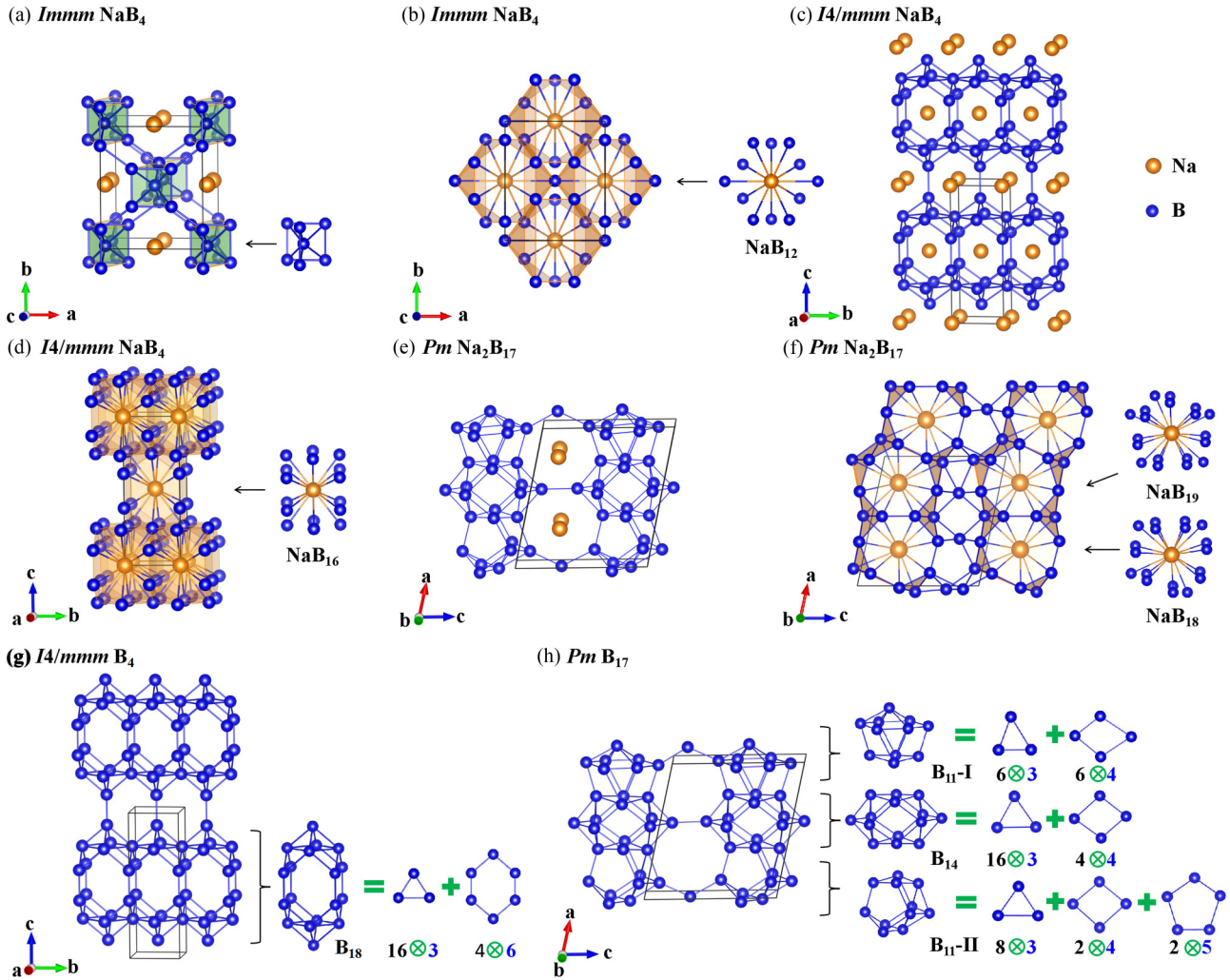
FIG. 2. Crystal structures of predicted Na-B compounds and B allotropes. (a) *Immm* NaB_4 with B_7 pentahedra at 50 GPa. (b) *Immm* NaB_4 with NaB_{12} units at 50 GPa. (c) *I4/mmm* NaB_4 at 100 GPa. (d) Each Na atom has a 16-fold coordination with B in *I4/mmm* NaB_4. (e) *Pm* Na_2B_{17} at 100 GPa. (f) Each Na atom is coordinated by 18 and 19 B atoms in *Pm* Na_2B_{17}. (g) *I4/mmm* B_4 at 1 atm. The 18-member B unit is shown in the inset, which consists of 16 trigons and 4 hexagons. (h) *Pm* B_{17} at 1 atm. Three different types of B units named as B_{11}-I, B_{14}, and B_{11}-II are included in *Pm* B_{17}. B_{11}-I includes six trigons and six irregular squares. B_{14} is composed of 16 trigons and 4 irregular squares. B_{11}-II contains eight trigons, two irregular squares, and two pentagons. In these structures, Na and B atoms are denoted in yellow and blue spheres, respectively.

phase is predicted to have an orthorhombic structure [space group *Immm*, 4 f.u. per cell, Fig. 2(a)]. There appears B_7 pentahedrons with B-B bond lengths of 1.65–1.80 Å at 50 GPa, and these pentahedrons make a B network via edge and face sharing. Each Na atom is 12-fold coordinated, with B forming a face-sharing Na-B polyhedra with Na-B bond lengths of 2.30–2.49 Å [Fig. 2(b)]. The high-pressure NaB_4 phase has a tetragonal structure [space group *I4/mmm*, 4 f.u. per cell, Fig. 2(c)], which is isostructural to LiB_4 [56]. Strikingly, it shows B_{18} icosahedrons [Fig. 2(g)], which are interconnected to form an open-channel frame with a B-B distance of 1.70–1.96 Å at 100 GPa. Notably, Na atoms sit at the center of the open channel and coordinate with 16 B atoms [Fig. 2(d)].

Na_2B_{17} stabilizes into a monoclinic structure [space group *Pm*, 1 f.u. per cell, Fig. 2(e)], consisting of three kinds of face-sharing B units, dubbed as B_{11}-I, B_{14}, and B_{11}-II [Fig. 2(h)]. The three B units interconnect with each other to form a

three-dimensional framework with an open channel along the *b* direction. The B-B bond length is 1.53–1.96 Å at 100 GPa. More interestingly, Na atoms form linear chains located in the skeletal channels. Notably, Na atom in Na_2B_{17} exhibits the highest coordination numbers (up to 19) among sodium borides. Electron localization function (ELF) [57] analysis shows that B-B bonds in three-dimensional frameworks of NaB_4 and Na_2B_{17} are covalent (Fig. S7); while the Na-B bonding is weakly ionic, which is also supported by the Bader charge analysis (Table S3). To analyze the relative bond strength between Na-B and B-B bonds, the integrated crystal orbital Hamilton populations (ICOHP) are employed as implemented in the LOBSTER package [58,59]. The resulting ICOHPs of Na-B and B-B pairs in *I4/mmm* NaB_4 are −0.033 and −3.410 eV/pair, respectively, indicating that the Na-B interaction is much weaker than that of B-B. A silicon allotrope, Si_{24}, has been obtained from Na_4Si_{24} through removing Na

atoms [18]. For comparison, the calculated ICOHPs of Na-Si and Si-Si pairs in Na_4Si_{24} are -0.066 and -2.544 eV/pair, respectively. This indicates that the Na-B interaction in NaB_4 is weaker than Na-Si in Na_4Si_{24}, whereas the B-B bond strength is stronger than Si-Si in Na_4Si_{24}. Similar results can be also seen in Pm Na_2B_{17} (Table S4).

Motivated by the unique structural characteristics of NaB_4 and Na_2B_{17} (covalent open B channels and Na located in the center of the open channel), we explore their energy and structural stability after removing Na atoms. The resulting structures, referred to as $I4/mmm$ B_4 and Pm B_{17}, are 0.24 and 0.25 eV/atom higher in energy than α-B_{12} [23] at 1 atm (Table S5), respectively. These are lower formation enthalpies than $P6/m$-Si_6 (0.35 eV/atom) [19] relative to Si in the diamond structure at 1 atm, indicating that they are metastable and could be synthesized at certain conditions. Their structures are comparable to the B sublattice in $I4/mmm$ NaB_4 and Pm Na_2B_{17} (their B-B covalent bonds are still maintained, Fig. S7), and are dynamically stable at ambient pressure [Figs. 3(a) and 3(b)]. Interestingly, $I4/mmm$ B_4 and Pm B_{17} are shown to be also mechanically stable (Table S6) [60]. In addition, we have also performed molecular dynamical simulations [61] at 1000 and 1500 K with a time step of 1.0 fs to verify their thermal stability. The snapshots of the resulting structures clearly indicate that $I4/mmm$ B_4 and Pm B_{17} also remain stable at these temperatures (Fig. S8), which supports their practical applicability.

Already known B allotropes at ambient and high pressures present a myriad of different structural characteristics with various interesting properties. For example, α-B_{12}, consisting of edging-sharing 20 boron trigons, is nonmetallic at ambient pressure [23]. High-pressure insulating ionic γ-B_{28} phase consists of cationic B_2 pairs and anionic icosahedral B_{12} containing 20 boron trigons, shows a reduction of the band gap with pressure similar to that of α-B_{12} [23]. Metallic α-Ga-type B, transformed from α-B_{12} above 74 GPa, which is regarded as the modification of B_{12} icosahedra [27], is a superhard material. Under higher pressure (>375 GPa) B_{10} phase presents a linear atomic chain combined with an isosceles triangle, exhibiting a high-T_c superconductivity of 44 K at 400 GPa [29]. Recently, several new metallic and hard B allotropes, termed as o-B_{24} (20.0 GPa), c-B_{56} (26.6 GPa), $m - B_{16}$ (56.2 GPa), and o-B_{16} (60.7 GPa) from ambient to high pressure up 120 GPa have been found, in which o-B_{24} has B_{12} icosahedra units, whereas B_{12} icosahedra in c-B_{56}, $m - B_{16}$, and o-B_{16} are absent [62]. More recently, it has been reported that t-B_{106} at ambient conditions is just slightly less stable than β-B [63], consisting of interstitial B atoms and interpenetrating icosahedra and α-B_{12} [64]. However, compared with boron units of the known B allotropes at ambient and high pressures that we have briefly described above, the clathrate boron structural units in $I4/mmm$ B_4 and Pm B_{17} we are predicting in this work are further dismembered into smaller B subunits, which usually induce the presence of interesting properties. In the $I4/mmm$ B_4, B_{18} icosahedron can be seen as the edge-sharing stacking of sixteen trigons and four hexagons [Fig. 2(g)], while in Pm B_{17}, B_{11}-I has six trigons and six irregular squares. B_{14} includes 16 trigons and 4 irregular squares. B_{11}-II is composed of eight trigons, two irregular squares, and two pentagons [Fig. 2(h)].
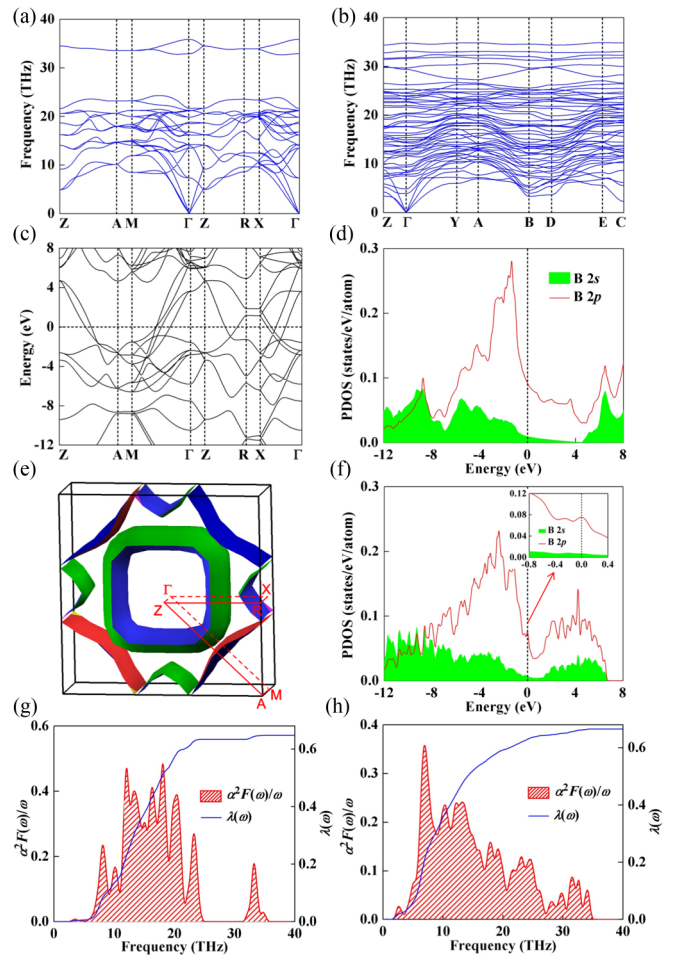

FIG. 3. Electronic and superconducting properties of $I4/mmm$ B_4 and Pm B_{17} at 1 atm. Phonon dispersion curves of (a) $I4/mmm$ B_4 and (b) Pm B_{17}. (c) Electronic band structure of $I4/mmm$ B_4. The horizontal dashed line indicates the Fermi level E_F. (d) PDOS of $I4/mmm$ B_4. The vertical dashed line indicates the Fermi level. (e) The Fermi surface for $I4/mmm$ B_4. The Fermi surface associated with each band crossing the Fermi energy is displayed in Fig. S10. (f) PDOS of Pm B_{17}. A close up of the PDOS around the van Hove singularity (vHs) near the E_F is illustrated in the inset of (f). Eliashberg spectral function $\alpha^2F(\omega)$ (red area) and frequency-dependent electron-phonon coupling parameters $\lambda(\omega)$ (blue line) of (g) $I4/mmm$ B_4 and (h) Pm B_{17}.

Considering the strong B-B covalent bonding, the three-dimensional B framework in $I4/mmm$ B_4 and Pm B_{17} and the excellent hardness in B-based compounds [65–68], we have also explored the hardness of the predicted new boron allotropes with the strain-stress method [69] and the Voigt-Reuss-Hill approximation [70]. Based on the empirical Vickers hardness model $H_v = 2.0(k^2G)^{0.585} - 3.0$, $k = G/B$, where G and B are the shear and bulk modulus [71], the calculated hardness values of $I4/mmm$ B_4 and Pm B_{17} are 27.3 and 26.8 GPa, respectively, indicating that they are good candidates as hard materials.

C. Electronic and superconducting properties

Much effort has been made to explore the superconductivity of B allotropes [72–75]. To be noted, two-dimensional

(2D) boron allotropes become superconducting due their unique structure and inherent metallity [72,73]. $I4/mmm$ B_4 and Pm B_{17} allotropes are metallic at ambient pressure, as shown in the electronic band structures and PDOS [Fig. S9 and Figs. 3(c), 3(d), and 3(f)]. Similar to $I4/mmm$ NaB_4 and Pm Na_2B_{17}, B $2p$ in $I4/mmm$ B_4 and Pm B_{17} allotropes has also a large contribution to their metallic character, with a strong hybridization between B $2s$ and B $2p$ orbitals [Figs. 3(d) and 3(f)], which plays a key role in stabilizing the covalent B networks. Additionally, there is a clear Fermi surface nesting in $I4/mmm$ B_4 along $Z \rightarrow A$ and $M \rightarrow \Gamma$ directions [Fig. 3(e)], with flatter bands along $A \rightarrow M$ and $R \rightarrow X$ [Fig. 3(c)], which induces high electronic density of states near the Fermi level [Figs. 3(d) and 3(f)]. There appears van Hove singularity [Fig. 3(f)] in Pm Na_2B_{17}. On the other hand, $I4/mmm$ B_4 and Pm B_{17} allotropes contain the novel B structural units, as described above. As these features might support the superconducting transition in these compounds, we have estimated their superconducting critical temperatures (T_c) using the Allen-Dynes modified McMillan equation [76–81] on the basis of Bardeen-Cooper-Schrieffer (BCS) [82] theory with adopting a typical Coulomb pseudopotential of $\mu^* = 0.1$. The superconducting temperatures of $I4/mmm$ B_4 and Pm B_{17} are predicted to be 19.8 and 15.4 K at ambient pressure, which are comparable to 2D B polymorphs (e.g., 18.7 K for β_{12} [74], 24.7 K for χ_3 [74], and 17.9 K for 2D boron layer [75]). The calculated electron-phonon coupling parameters λ of $I4/mmm$ B_4 and Pm B_{17} at 1 atm are 0.65 and 0.67, respectively, comparable to 0.61 in MgB_2 [83]. As clearly revealed in Fig. 3(g), the electron-phonon coupling (EPC) constant of $I4/mmm$ B_4 mainly arises from the contribution of low-frequency phonon modes below 23.9 THz, giving the dominant contribution (97.8%) to the integral EPC constant λ. The same is observed in Pm B_{17}, in which low-frequency vibrations below 27.1 THz contribute 96.7% of the total λ [Fig. 3(h)]. Therefore, the superconducting mechanism is quite similar to that of the superconducting Li_6P electride [84], but different from the high-frequency H-derived vibrations of high-T_c H_3S [7,12], H_3Se [85], and $CaYH_{12}$ [86] superconductors and intermediate-frequency H-derived vibrations of H_4Te [87].

IV. CONCLUSIONS

In summary, four hitherto unknown Na-B compounds (i.e., Na_3B_2, Na_2B_3, NaB_4, and Na_2B_{17}) are identified with first-principle swarm-intelligence structural search calculations. The arrangements of B atoms in these compounds evolve sequentially with increasing the B content from one-dimensional B linear chains to B_6 octahedra, B_7 pentahedra, and three-dimensional B frameworks. Removing Na atoms from $I4/mmm$ NaB_4 and Pm NaB_{17}, two metallic $I4/mmm$ B_4 and Pm B_{17} allotropes become very stable at ambient conditions. Besides being potential hard compounds, among the already known three-dimensional boron allotropes, they show the highest superconducting transition temperatures of 19.8 and 15.4 K. Our work provides an effective way to get superconducting boron allotropes.

[1] C. J. Pickard, I. Errea, and M. I. Eremets, Annu. Rev. Condens. Matter Phys. **11**, 57 (2020).

[2] A. R. Oganov, C. J. Pickard, Q. Zhu, and R. J. Needs, Nat. Rev. Mater. **4**, 331 (2019).

[3] E. Zurek and T. Bi, J. Chem. Phys. **150**, 050901 (2019).

[4] D.-H. Lee, Annu. Rev. Condens. Matter Phys. **9**, 261 (2018).

[5] L. Zhang, Y. Wang, J. Lv, and Y. Ma, Nat. Rev. Mater. **2**, 17005 (2017).

[6] A. Jain, Y. Shin, and K. A. Persson, Nat. Rev. Mater. **1**, 15004 (2016).

[7] A. P. Drozdov, M. I. Eremets, I. A. Troyan, V. Ksenofontov, and S. I. Shylin, Nature (London) **525**, 73 (2015).

[8] A. P. Drozdov, P. P. Kong, V. S. Minkov, S. P. Besedin, M. A. Kuzovnikov, S. Mozaffari, L. Balicas, F. F. Balakirev, D. E. Graf, V. B. Prakapenka, E. Greenberg, D. A. Knyazev, M. Tkacz, and M. I. Eremets, Nature (London) **569**, 528 (2019).

[9] M. Somayazulu, M. Ahart, A. K. Mishra, Z. M. Geballe, M. Baldini, Y. Meng, V. V. Struzhkin, and R. J. Hemley, Phys. Rev. Lett. **122**, 027001 (2019).

[10] L. Gao, Y. Y. Xue, F. Chen, Q. Xiong, R. L. Meng, D. Ramirez, C. W. Chu, J. H. Eggert, and H. K. Mao, Phys. Rev. B **50**, 4260 (1994).

[11] Y. Li, J. Hao, H. Liu, Y. Li, and Y. Ma, J. Chem. Phys. **140**, 174712 (2014).

[12] D. Duan, Y. Liu, F. Tian, D. Li, X. Huang, Z. Zhao, H. Yu, B. Liu, W. Tian, and T. Cui, Sci. Rep. **4**, 6968 (2014).

[13] H. Liu, I. I. Naumov, R. Hoffmann, N. W. Ashcroft, and R. J. Hemley, Proc. Natl. Acad. Sci. USA **114**, 6990 (2017).

[14] Y. Sun, J. Lv, Y. Xie, H. Liu, and Y. Ma, Phys. Rev. Lett. **123**, 097001 (2019).

[15] J. J. Hamlin, Nature (London) **569**, 491 (2019).

[16] P. V Zinin, L. C. Ming, H. A. Ishii, R. Jia, T. Acosta, and E. Hellebrand, J. Appl. Phys. **111**, 114905 (2012).

[17] T. Irifune, A. Kurio, S. Sakamoto, T. Inoue, and H. Sumiya, Nature (London) **421**, 599 (2003).

[18] D. Y. Kim, S. Stefanoski, O. O. Kurakevych, and T. A. Strobel, Nat. Mater. **14**, 169 (2014).

[19] H.-J. Sung, W. H. Han, I.-H. Lee, and K. J. Chang, Phys. Rev. Lett. **120**, 157001 (2018).

[20] B. Albert and H. Hillebrecht, Angew. Chemie Int. Ed. **48**, 8640 (2009).

[21] T. Ogitsu, E. Schwegler, and G. Galli, Chem. Rev. **113**, 3425 (2013).

[22] K. Shirai, Jpn. J. Appl. Phys. **56**, 05FA06 (2017).

[23] A. R. Oganov, J. Chen, C. Gatti, Y. Ma, Y. Ma, C. W. Glass, Z. Liu, T. Yu, O. O. Kurakevych, and V. L. Solozhenko, Nature (London) **457**, 863 (2009).

[24] X.-L. He, X. Shao, T. Chen, Y.-K. Tai, X.-J. Weng, Q. Chen, X. Dong, G. Gao, J. Sun, X.-F. Zhou, Y. Tian, and H.-T. Wang, Phys. Rev. B **99**, 184111 (2019).

[25] M. I. Eremets, V. V Struzhkin, H. Mao, and R. J. Hemley, Science **293**, 272 (2001).

[26] J. Zhao and J. P. Lu, Phys. Rev. B **66**, 092101 (2002).

[27] U. Häussermann, S. I. Simak, R. Ahuja, and B. Johansson, Phys. Rev. Lett. **90**, 065701 (2003).

[28] Y. Ma, J. S. Tse, D. D. Klug, and R. Ahuja, Phys. Rev. B **70**, 214107 (2004).

[29] D. Li, K. Bao, F. Tian, X. Jin, D. Duan, Z. He, B. Liu, and T. Cui, RSC Adv. **4**, 203 (2014).

[30] W. Zhang, A. R. Oganov, A. F. Goncharov, Q. Zhu, S. E. Boulfelfel, A. O. Lyakhov, E. Stavrou, M. Somayazulu, V. B. Prakapenka, and Z. Konôpková, Science **342**, 1502 (2013).

[31] M. Miao, Nat. Chem. **5**, 846 (2013).

[32] J. Lin, Z. Zhao, C. Liu, J. Zhang, X. Du, G. Yang, and Y. Ma, J. Am. Chem. Soc. **141**, 5409 (2019).

[33] B. Albert, Angew. Chem. Int. Ed. **37**, 1117 (1998).

[34] Y. Zhong, C.-H. Hu, D. Wang, and H.-Y. Zhou, J. Alloys Compd. **731**, 323 (2018).

[35] X.-L. He, X. Dong, Q. S. Wu, Z. Zhao, Q. Zhu, A. R. Oganov, Y. Tian, D. Yu, X.-F. Zhou, and H.-T. Wang, Phys. Rev. B **97**, 100102(R) (2018).

[36] Y. Wang, J. Lv, L. Zhu, and Y. Ma, Phys. Rev. B **82**, 094116 (2010).

[37] Y. Wang, J. Lv, L. Zhu, and Y. Ma, Comput. Phys. Commun. **183**, 2063 (2012).

[38] G. Kresse and J. Furthmüller, Phys. Rev. B **54**, 11169 (1996).

[39] P. Hohenberg and W. Kohn, Phys. Rev. **136**, B864 (1964).

[40] W. Kohn and L. J. Sham, Phys. Rev. **140**, A1133 (1965).

[41] P. E. Blöchl, Phys. Rev. B **50**, 17953 (1994).

[42] P. Blaha, K. Schwarz, P. Sorantin, and S. B. Trickey, Comput. Phys. Commun. **59**, 399 (1990).

[43] J. P. Perdew, K. Burke, and M. Ernzerhof, Phys. Rev. Lett. **77**, 3865 (1996).

[44] J. P. Perdew, J. A. Chevary, S. H. Vosko, K. A. Jackson, M. R. Pederson, D. J. Singh, and C. Fiolhais, Phys. Rev. B **46**, 6671 (1992).

[45] H. J. Monkhorst and J. D. Pack, Phys. Rev. B **13**, 5188 (1976).

[46] P. Giannozzi, S. Baroni, N. Bonini, M. Calandra, R. Car, C. Cavazzoni, D. Ceresoli, G. L. Chiarotti, M. Cococcioni, I. Dabo, A. Dal Corso, S. de Gironcoli, S. Fabris, G. Fratesi, R. Gebauer, U. Gerstmann, C. Gougoussis, A. Kokalj, M. Lazzeri, L. Martin-Samos, N. Marzari, F. Mauri, R. Mazzarello, S. Paolini, A. Pasquarello, L. Paulatto, C. Sbraccia, S. Scandolo, G. Sclauzero, A. P. Seitsonen, A. Smogunov, P. Umari, and R. M. Wentzcovitch, J. Phys. Condens. Matter **21**, 395502 (2009).

[47] See Supplemental Material at http://link.aps.org/supplemental/10.1103/PhysRevB.101.174507 for computational details. Phonon dispersion curves, projected phonon density of states (PHDOS), electronic band structures, projected density of states

(PDOS), and electron localization function (ELF) of predicted stable Na-B phases. ELF, mechanical, and superconducting properties of $I4/mmm$ B$_4$ and Pm B$_{17}$.

[48] J. Feng, R. G. Hennig, N. W. Ashcroft, and R. Hoffmann, Nature (London) **451**, 445 (2008).

[49] C. S. Barrett, Acta Crystallogr. **9**, 671 (1956).

[50] M. Hanfland, I. Loa, and K. Syassen, Phys. Rev. B **65**, 184109 (2002).

[51] F. Peng, M. Miao, H. Wang, Q. Li, and Y. Ma, J. Am. Chem. Soc. **134**, 18599 (2012).

[52] C.-H. Hu, A. R. Oganov, Q. Zhu, G.-R. Qian, G. Frapper, A. O. Lyakhov, and H.-Y. Zhou, Phys. Rev. Lett. **110**, 165504 (2013).

[53] S. Zhang, J. Lin, Y. Wang, G. Yang, A. Bergara, and Y. Ma, J. Phys. Chem. C **122**, 12022 (2018).

[54] K. Parlinski, Z. Q. Li, and Y. Kawazoe, Phys. Rev. Lett. **78**, 4063 (1997).

[55] A. Togo, F. Oba, and I. Tanaka, Phys. Rev. B **78**, 134106 (2008).

[56] A. Hermann, A. McSorley, N. W. Ashcroft, and R. Hoffmann, J. Am. Chem. Soc. **134**, 18606 (2012).

[57] A. D. Becke and K. E. Edgecombe, J. Chem. Phys. **92**, 5397 (1990).

[58] R. Dronskowski and P. E. Bloechl, J. Phys. Chem. **97**, 8617 (1993).

[59] S. Maintz, V. L. Deringer, A. L. Tchougréeff, and R. Dronskowski, J. Comput. Chem. **37**, 1030 (2016).

[60] Z. J. Wu, E. J. Zhao, H. P. Xiang, X. F. Hao, X. J. Liu, and J. Meng, Phys. Rev. B **76**, 054115 (2007).

[61] G. J. Martyna, M. L. Klein, and M. Tuckerman, J. Chem. Phys. **97**, 2635 (1992).

[62] C. Fan, J. Li, and L. Wang, Sci. Rep. **4**, 6786 (2014).

[63] M. J. van Setten, M. A. Uijttewaal, G. A. de Wijs, and R. A. de Groot, J. Am. Chem. Soc. **129**, 2458 (2007).

[64] Q. An, K. Madhav Reddy, K. Y. Xie, K. J. Hemker, and W. A. Goddard, Phys. Rev. Lett. **118**, 159902(E) (2017).

[65] H.-Y. Chung, M. B. Weinberger, J. B. Levine, A. Kavner, J.-M. Yang, S. H. Tolbert, and R. B. Kaner, Science **316**, 436 (2007).

[66] Q. Gu, G. Krauss, and W. Steurer, Adv. Mater. **20**, 3620 (2008).

[67] R. Mohammadi, A. T. Lech, M. Xie, B. E. Weaver, M. T. Yeung, S. H. Tolbert, and R. B. Kaner, Proc. Natl. Acad. Sci. USA **108**, 10958 (2011).

[68] H. Gou, N. Dubrovinskaia, E. Bykova, A. A. Tsirlin, D. Kasinathan, W. Schnelle, A. Richter, M. Merlini, M. Hanfland, A. M. Abakumov, D. Batuk, G. Van Tendeloo, Y. Nakajima, A. N. Kolmogorov, and L. Dubrovinsky, Phys. Rev. Lett. **111**, 157002 (2013).

[69] Y. Le Page and P. Saxe, Phys. Rev. B **65**, 104104 (2002).

[70] R. Hill, Proc. Phys. Soc. Sect. A **65**, 349 (1952).

[71] X.-Q. Chen, H. Niu, D. Li, and Y. Li, Intermetallics **19**, 1275 (2011).

[72] E. S. Penev, A. Kutana, and B. I. Yakobson, Nano Lett. **16**, 2522 (2016).

[73] Y. Zhao, S. Zeng, and J. Ni, Phys. Rev. B **93**, 014502 (2016).

[74] M. Gao, Q.-Z. Li, X.-W. Yan, and J. Wang, Phys. Rev. B **95**, 024505 (2017).

[75] T. Chen, Q. Gu, Q. Chen, X. Wang, C. J. Pickard, R. J. Needs, D. Xing, and J. Sun, Phys. Rev. B **101**, 054518 (2020).

[76] W. L. McMillan, Phys. Rev. **167**, 331 (1968).

[77] P. B. Allen and R. C. Dynes, Phys. Rev. B **12**, 905 (1975).

[78] J. P. Carbotte, Rev. Mod. Phys. **62**, 1027 (1990).

[79] L. N. Oliveira, E. K. U. Gross, and W. Kohn, Phys. Rev. Lett. **60**, 2430 (1988).

[80] M. Lüders, M. A. L. Marques, N. N. Lathiotakis, A. Floris, G. Profeta, L. Fast, A. Continenza, S. Massidda, and E. K. U. Gross, Phys. Rev. B **72**, 024545 (2005).

[81] M. A. L. Marques, M. Lüders, N. N. Lathiotakis, G. Profeta, A. Floris, L. Fast, A. Continenza, E. K. U. Gross, and S. Massidda, Phys. Rev. B **72**, 024546 (2005).

[82] J. Bardeen, L. N. Cooper, and J. R. Schrieffer, Phys. Rev. **108**, 1175 (1957).

[83] H. J. Choi, D. Roundy, H. Sun, M. L. Cohen, and S. G. Louie, Phys. Rev. B **66**, 020513(R) (2002).

[84] Z. Zhao, S. Zhang, T. Yu, H. Xu, A. Bergara, and G. Yang, Phys. Rev. Lett. **122**, 097002 (2019).

[85] S. Zhang, Y. Wang, J. Zhang, H. Liu, X. Zhong, H.-F. Song, G. Yang, L. Zhang, and Y. Ma, Sci. Rep. **5**, 15433 (2015).

[86] X. Liang, A. Bergara, L. Wang, B. Wen, Z. Zhao, X.-F. Zhou, J. He, G. Gao, and Y. Tian, Phys. Rev. B **99**, 100505(R) (2019).

[87] X. Zhong, H. Wang, J. Zhang, H. Liu, S. Zhang, H.-F. Song, G. Yang, L. Zhang, and Y. Ma, Phys. Rev. Lett. **116**, 057002 (2016).